Available online at www.sciencerepository.org

Science Repository

Research Article

Albutate-1, a Novel Long-Circulating Radiotracer Targeting the Somatostatin Receptor Subtype 2

Sandra van Tiel[1*], Theodosia Maina[2], Berthold Nock[2], Mark Konijnenberg[1], Erik de Blois[1], Yann Seimbille[1,3], Monique Bernsen[1] and Marion de Jong[1]

[1]*Department of Radiology & Nuclear Medicine, Erasmus MC, Rotterdam, The Netherlands*
[2]*Molecular Radiopharmacy, INRASTES NCSR 'Demokritos', Athens, Greece*
[3]*Division of Life Sciences, TRIUMF, Vancouver, Canada*

ARTICLE INFO

Article history:
Received: 5 January, 2021
Accepted: 20 January, 2021
Published: 3 March, 2021

Keywords:
DOTA-TATE
Albutate-1
albumin binding domain
biodistribution
dosimetry

ABSTRACT

Currently, radiolabeled DOTA-[Tyr^3]-octreotate (DOTA-TATE) is most commonly used in the clinic to image and treat neuroendocrine tumors. To further improve tumor uptake, and thus treatment, the amount of radiotracer that can accumulate in the tumor might be increased by prolonging the blood circulation time of the radiotracer. To achieve this, we designed Albutate-1, with both DOTA and an albumin-binding domain coupled to TATE via a suitable linker. The aim of this study was to determine the characteristics of the novel radiotracer Albutate-1. A competition binding assay was performed using [^{111}In]In-DOTA-TATE on fresh-frozen SSTR2$^+$ tumor sections. *In vitro* cell-uptake and internalization of [^{111}In]In-Albutate-1 and [^{111}In]In-DOTA-TATE were determined. The stability of [^{177}Lu]Lu-Albutate-1 was tested. A biodistribution study was performed to provide tumor and organ uptake of [^{177}Lu]Lu-Albutate-1. The biodistribution data was used to determine time-activity curves and the radiation dose for each organ and the tumor. The *in vitro* IC_{50} value of Albutate-1 was 1.2 nM. A higher amount of the tracer was found in the intracellular fraction than in the membrane fraction ([^{111}In]In-Albutate-1 14.0 vs 1.9% of the added amount; [^{111}In]In-DOTA-TATE 11.0 vs 1.5% of the added amount). After radiolabeling [^{111}In] In-Albutate-1 was stable up to 3 days (93.1-88.9%) in labeling solution and very stable in mouse serum (90-94%) for at least 24 h. *In vivo*, [^{177}Lu]Lu-Albutate-1 was cleared slowly from the circulation (1 h p.i. 58%ID/g, 168h p.i. 2%ID/g). The addition of an albumin-binding domain to DOTA-TATE extended the blood circulation to $T_{1/2}$= 27.5h. The tumor absorbed dose was raised to 1455 mGy/MBq. Bone marrow, the dose-limiting organ in the mouse spine, unfortunately, received 765 mGy/MBq. All other organs also received a high radiation dose, reducing the therapeutic index.

Introduction

Neuroendocrine tumors (NETs) originate mostly from gastroenteropancreatic (GEP) and bronchial tissue [1]. NETs are rare tumors and are often metastasized at the time of diagnosis [2]. NETs typically express high levels of somatostatin receptor subtype 2 (SSTR2). Hence the SSTR2 represents an excellent target for diagnosis and treatment of the disease using high-affinity radiolabeled peptide ligands. For nuclear imaging of NETs [^{111}In]In-DTPA-octreotide (Octreoscan®) has long been the radiotracer of choice. With the aim to improve diagnostic sensitivity, new octreotide analogs were developed that are suitable for labeling with gallium-68 and fluor-18 and applied for positron emission tomography (PET), for example, [^{68}Ga]Ga-DOTA-Tyr^3-octreotide ([^{68}Ga]Ga-DOTA-TOC), [^{68}Ga]Ga-DOTA-Tyr^3-octreotate ([^{68}Ga]Ga-DOTA-TATE), [^{68}Ga]Ga-DOTA-1-Nal^3-octreotide ([^{68}Ga]Ga-DOTA-NOC) and [^{18}F]F-FET-βAG-TOCA [3, 4].

Correspondence to: Sandra van Tiel, Department of Radiology & Nuclear Medicine, Erasmus MC, Rotterdam, The Netherlands; Tel: +31107044198; E-mail: s.vantiel@erasmusmc.nl

http://dx.doi.org/10.31487/j.JNMRS.2021.01.01

For therapy two radiotracers are most commonly used, [^{90}Y]Y-DOTA-Tyr^3-octreotide and ([^{177}Lu]Lu-DOTA-Tyr^3-octreotate ([^{177}Lu]Lu-DOTA-TATE) [5-7]. Disease-control rates for these therapies are between 68-94% [8]. An increase in progression-free survival and overall survival was reported when compared to the values after chemotherapy and targeted therapy with everolimus and sunitinib [9]. An advantage of [^{90}Y]Y-DOTA-octreotide or [^{177}Lu]Lu-DOTA-TATE therapy is that prior to the therapy the target (SSTR2) can be identified and quantified using PET (^{68}Ga) or SPECT (^{111}In) with the tracer. This way, the therapeutic dose delivered to the tumor can be calculated accurately [8, 10].

As there is no 100% complete response rate, there is room to enhance the therapeutic efficacy with e.g. higher doses of the radiopharmaceutical, but this is restricted by concomitant higher radiation doses to other organs. The organs at risk for long-term toxicity are predominantly the kidneys and the bone marrow. The renal radiation dose can, however, be reduced by co-infusion of cationic amino acids (i.e. lysine, arginine) or with the use of a gelatin-based plasma expander (Gelofusine), leaving the bone marrow, the main dose-limiting organ for treatment [11, 12]. The blood clearance of [^{177}Lu]Lu-DOTA-TATE in humans is rapid (<10%ID in blood at 3 h post-injection) [13]. Reversible plasma protein-binding represents a promising strategy to prolong the circulation time and thus improve the target-localization of rapidly clearing drugs, including small-size radiopharmaceuticals [14]. A series of albumin-binding entities have been proposed as pharmacokinetic modifiers to enhance the accumulation of small, radiolabeled vectors on target-sites. Amongst these agents is Evans Blue (EB). EB and its analogs exhibit a modest affinity for serum albumin [15-17].

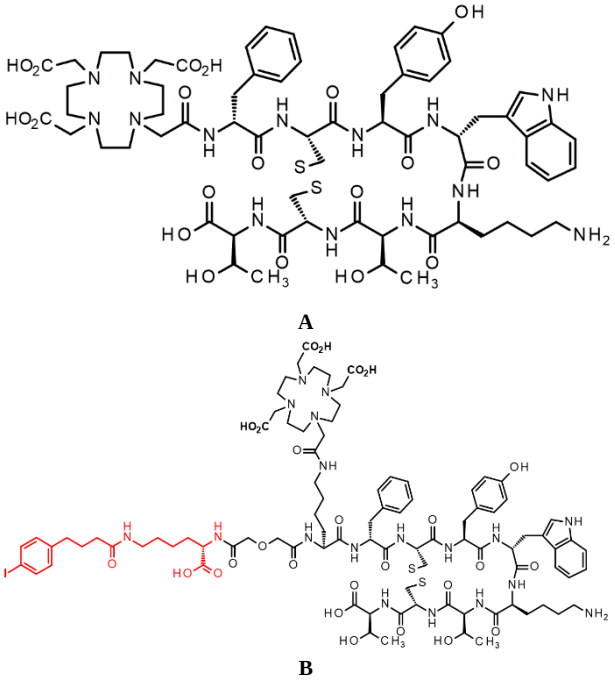

Figure 1: Chemical structure of **A)** DOTA-TATE and **B)** Albutate-1, carrying the albumin-binding domain (4-(p-iodophenyl) butyric acid-DLys) to TATE via the diglycolate-Lys (DOTA) linker with DOTA attached on the pendant ε-amine of Lys.

Another agent is 4-(p-iodophenyl) butyric acid-Dlys (I-PBA), previously discovered from a DNA-encoded chemical library, has been used for such purposes. After coupling I-PBA with antibody fragments, folic acid radioconjugates, DOTA-based bisphosphonates, and PSMA-directed radioligands, the desired effect of enhancing blood circulation was shown for the modified compounds [18-24]. Hence, as a first effort to prolong the blood circulation time of [^{177}Lu]Lu-DOTA-TATE to better match the half-life of ^{177}Lu, we have selected I-PBA-Dlys for coupling to DOTA-TATE. The above-described studies have shown that conjugation of I-PBA-Dlys and DOTA to a lysine is possible without abolishing the interaction of the molecule with albumin. Following this approach, we have incorporated I-PBA-Dlys and a diglycolic acid-Dlys spacer carrying DOTA on its pendant ε-amine of Lys at the N-terminus of TATE as depicted in (Figure 1) (Analytical data sheet in supporting information). We studied its binding capacity to the SSTR2 *in vitro* and its *in vivo* behaviour in tumor-bearing mice, thereby also focusing on potential radiotoxicity in normal organs.

Materials and Methods

I Labeling of DOTA-TATE and Albutate-1

A typical reaction mixture for radiolabeling is 60 MBq of ^{177}Lu- (Lu-Mark, 80 GBq/mL, AAA, IDB Holland) or $^{111}InCl_3$ (740 MBq/mL, CURIUM) in 0.01-0.05 M HCl, 1 nmol peptide dissolved in Milli-Q water, and sodium acetate as buffer (<2μL of 2.5M), 10μL of ascorbic acid and gentisic acid (0.05 M) and 10 μL of ethanol in a final volume of 140 μL (final pH 4-4.5). Labelling solutions were heated for 20 min 90ºC in a heating block [25]. Quality control was performed after the addition of 5 μL 4 mM DTPA post radiolabeling. Quality control includes radiochemical yield (RCY) of In-111 or Lu-177 as measured by ITLC-SG and radiochemical purity (RCP) of radiolabeled peptides were measured by HPLC [26]. For each measurement of RCY, two strips were prepared, each being 1 cm wide and 10 cm long. On each strip an aliquot (~ 1 μL) of the sample of interest was applied on circa 1 cm from the bottom of the strip, after which the strip was placed into the eluent. After the eluent had been displaced to the top of the strip, the strip was cut into two parts. Each piece was measured in a gamma counter separately and RCY was calculated. RCP was determined at the end of the synthesis. TLC-SG samples and calculate RCY.

RCP measurements were conducted with an instrument setup that consisted of a Waters Alliance HPLC system (Etten-leur, The Netherlands) and radio measurement setup. HPLC system is comprised of an e2690/5 separation module, W2998 PDA detector in combination with a Waters symmetry C18 column (5 μm, 4.6 mm × 250 mm) (Etten-Leur, The Netherlands). Radio measurements were performed with an 1″ NaI(Tl) Scionix crystal (Bunnik, The Netherlands) connected to a Canberra Osprey multichannel analyser and signal amplifier (Zellik, Belgium). The signal connection between radio measurement setup and HPLC was obtained via a Waters E-satin Interface. Samples for analysis (also for stability studies) were diluted to a volumetric activity of 0.8-1.0 MBq per 100 μL for Lu-177 and 0.2-0.3 MBq for In-111 and separated using 0.1% trifluoroacetic acid (TFA, eluents A) and methanol (Eluents B) in combination with the gradient profile shown in (Figure 2).

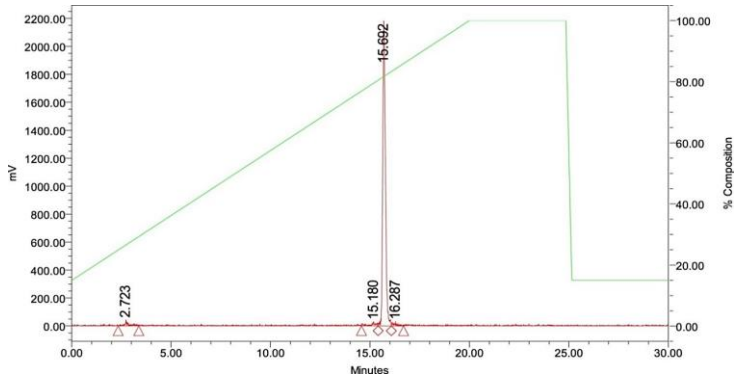

Figure 2: Gradient profile.

II Stability Study

[^{111}In]In-Albutate-1 was added (18 µL, 50 MBq/nmol) to 300 µL of mouse plasma and this mixture was incubated at 37°C for 1 hour in an Eppendorf ThermoMixer® heating block (Eppendorf, Nijmegen, The Netherlands). After incubation of the radioligand, with different time interval (1,4, and 24h), with mouse serum, precipitation was performed with ethanol (1:1 v/v) and after centrifugation (5 min, ~10.000 g), plasma stability of [^{111}In]In-Albutate-1 was measured by HPLC at 1, 4 and 24 h. The stability of [^{111}In]In-Albutate-1 in the labeling buffer was also determined by HPLC at 1 h, 1, 2 and 3 days.

III Competition Binding Assay

A competition binding assay was performed in triplicate on SSTR2-positive H69 tumor cryosections (10 µm). The sections were incubated for 1 h with [^{111}In]In-DOTA-TATE (100 µL, 10^{-9} M) in the presence of unlabeled Albutate-1 (range: 10^{-6}-10^{-12} M). After incubation, excess radiotracer was removed and the sections were exposed to super-resolution phosphor screens for 3 days (PerkinElmer, Rotterdam, The Netherlands). Binding of [^{111}In]In-DOTA-TATE to SSTR2-containing regions was quantified using OptiQuant (Perkin Elmer, Rotterdam, The Netherlands) and expressed in density light units/mm^2 (DLU/mm^2). Binding of 10^{-12} M [^{111}In]In-DOTA-TATE to the tissue slices was set at 100%, and the percentage of binding relative to the unblocked tissue sample was calculated for the (partially) blocked tissue sections. These values were used to determine the IC_{50} value of unlabeled Albutate-1.

IV Cell-Uptake and Internalization of [^{111}In]In-Albutate-1 and [^{111}In]In-DOTA-TATE

Uptake and internalization of the tracers in adhering U2OS-SSTR2 cells was determined as previously reported [27]. U2OS-SSTR2 cells were cultured in Dulbecco modified Eagle medium (Lonza, Geleen, The Netherlands), supplemented with 10% v/v fetal bovine serum (Biowest, Amsterdam, The Netherlands) and 5 mL of penicillin (5,000 units/mL)/streptomycin (5,000 µg/mL) (Sigma Aldrich), at 3°C and 5% CO_2. Twenty-four hours after seeding (12-well plates, 8 × 10^4 cells/well), the cells were incubated with 10^{-9} M of [^{111}In]In-Albutate-1 or [^{111}In]In-DOTA-TATE in 1 mL of culture medium for 1 h at 37°C. Cellular uptake was stopped by removing the medium from the cells, followed by washing twice with 2 mL phosphate-buffered saline (PBS; Gibco, Carlsbad, USA). By incubating cells for 10 min with an acid solution (50 mM glycine and 100 mM NaCl, pH 2.8) the membrane-bound radiotracer fraction was separated from the intracellular fraction. Then the cells were lysed using 0.1 M NaOH to collect the internalized fraction of the radiotracer. Activity levels of both fractions were counted in a γ-counter (1480 WIZARD automatic γ counter: PerkinElmer) using a radionuclide-specific energy window, a counting time of 60 s, and a counting error of 5% or less. Data are expressed as a percentage of added activity (%AA). The experiment was performed in triplicate and gamma-counter measurements were corrected for decay.

V *In Vivo* Biodistribution

The *in vivo* experiments were done according to the ARRIVE guidelines and approved by the Animal Welfare Committee of the Erasmus MC (AVD101002017867) [28]. *In vivo* biodistribution studies were performed for [^{177}Lu]Lu-Albutate-1. Male Balb/c nu/nu mice of 4-5 weeks old (Envigo, Horst, The Netherlands) were inoculated subcutaneously with 4 X 10^6 H69 tumor cells. When a tumor volume of on average 200 mm^3 was reached, the mice were injected with 30 MBq/240 pmol of [^{177}Lu]Lu-Albutate-1 intravenously via the tail vein. Two minutes prior to this injection 4 mg Gelofusine (B. Braun Medical BV, Oss, The Netherlands) was injected i.v. to reduce renal uptake [12]. Four mice were injected with block; 50 ug Albutate-1, 1 minute prior to an injection with gelofusin and 30 MBq/240 pmol of [^{177}Lu]Lu-Albutate-1. Mice were euthanized at different time points (1, 24, 48, 72 and 168 h, n=4 per time point) post-injection (p.i.). Blood, various organs and tumor were collected, weighed and radioactivity contained in the tissue samples was measured in a gamma counter (Wallac, 1480 Wizard 3", PerkinElmer, Turku, Finland). The percentage injected dose per gram of tissue (%ID/g) was calculated. Mice were housed at the Experimental Animal Facility of the Erasmus MC with a 12 h light-dark regimen in individually ventilated cages including extensive cage enrichment. The mice received acidified tap water and standard chow *ad libitum*. *In vivo* studies with [^{177}Lu]Lu-DOTA-TATE were previously performed at our department [29-32].

VI Dosimetry

The biodistribution data for [^{177}Lu]Lu-Albutate-1 was used to determine time-activity curves (TAC) for each organ and the tumor. A single compartment distribution model was assumed for the fit of the TAC data with a bi-exponential curve A(t):

$$A(t) = A_{max}\left(\exp(-\lambda_{clr}t) - \exp(-\lambda_{upt}t)\right)$$

with coefficients for uptake ($\lambda_{upt} = \ln(2)/T_{upt}$) proceeding with a half-life of T_{upt} and for clearance ($\lambda_{clr} = \ln(2)/T_{clr}$), proceeding with a clearance half-life of T_{clr}. The blood TAC was fitted with a single exponential function. The total number of disintegrations Ã in each organ was calculated by integration to infinity of the exponential curves multiplied with the ^{177}Lu decay curve. The absorbed doses were determined according to the MIRD equation $D_k = \sum_h \tilde{A}_h \times S(k \leftarrow h)$. The S-values for ^{177}Lu in a 22 g mouse were obtained from Monte Carlo calculations in the Realistic Moby phantom, kindly provided by Erik Larsson [33]. The blood contents in each bone marrow compartment were determined with the blood TAC and the marrow cellularity, according to Colvin *et al*. [34]. The distribution of the blood Ã in each marrow compartment was based on the fractional cellularity C_{BM}.

VII Statistics

Prism software (version 5.01, GraphPad Software) was used for statistical analyses. P values < 0.05 were considered statistically significant. To compare the uptake and internalization of both tracers, we used a two-tailed student t-test. Curve fitting for kinetic profiling was performed according to the least/square fit with the Pearson R^2 to quantify its goodness of fit.

Results

I Stability Study

After radiolabeling [^{111}In]In-Albutate-1 was stable up to 3 days (day 1 93.1% - day 3 88.9%) in the labeling buffer. [^{111}In]In-Albutate-1 was found very stable in mouse serum (between 90-94% within 24h) (Figure 3).

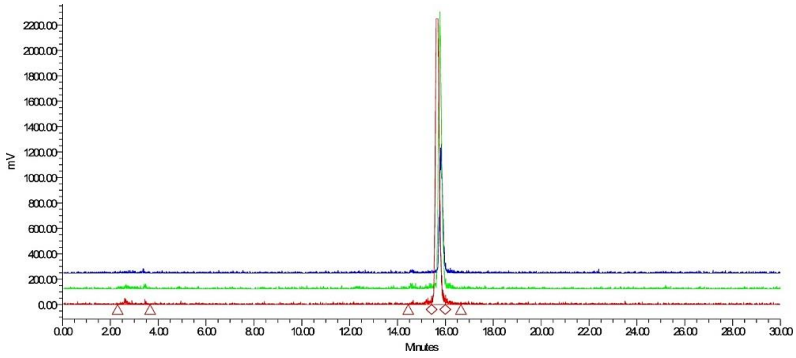

Figure 3: Stability of 0.2-0.3 MBq/100 µL [^{111}In]In-Albutate-1 injected after incubation 1h (red), 4h (green), 24h (blue) after injection in serum.

II Binding Affinity of Albutate-1

[^{111}In]In-DOTA-TATE was displaced from somatostatin binding sites in H69 tumor sections by Albutate-1 in a monophasic, dose-dependent manner. The IC_{50} value calculated for Albutate-1 was 1.2 nM (95% CI: 0.21nM to 6.99nM) (Figure 4).

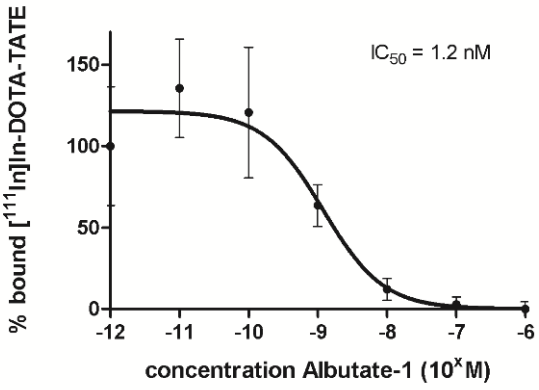

Figure 4: Displacement curve of [^{111}In]In-DOTA-TATE from somatostatin binding sites on H69 tumor sections by increasing concentrations of Albutate-1.

III Cell-Uptake and Internalization of [^{111}In]In-Albutate-1 and [^{111}In]In-DOTA-TATE

The internalization rate of [^{111}In]In-Albutate-1 was assessed in comparison to that of [^{111}In]In-DOTA-TATE (Figure 5). The total uptake was respectively 15.97 ± 0.58% AA and 12.81 ± 1.1% AA ($p<0.05$). We also distinguished between the internalized (intracellular fraction) and the membrane-bound fraction (membrane fraction). Most radioactivity was found to be internalized: 88.25 ± 0.87% for [^{111}In]In-DOTA-TATE and 88.3 ± 0.99% for [^{111}In]In-Albutate-1 ($p=0.97$). Both [^{111}In]In-Albutate-1 and [^{111}In]In-DOTA-TATE could be blocked by co-incubation with an excess of their corresponding unlabeled peptide.

IV *In Vivo* Biodistribution

Biodistribution studies were performed at 5 different time points after injection of [^{177}Lu]Lu-Albutate-1 (30 MBq/240 pmol) (Figure 6). At 1 h post-injection the activity level of [^{177}Lu]Lu-Albutate-1 in the blood was 58.59 ± 6.30%ID/g and gradually decreased down to 2.51 ± 0.22%ID/g at 168 h with a T_{clr} of 27.5 ± 2.6 h. (Figure 7). The measured tumor uptake was 7.07 ± 1.87%ID/g at 1 h p.i.. At 24 h p.i. the tumor uptake was 24.42 ± 1.44%ID/g and reaching 8.82 ± 1.92%ID/g at 168 h p.i. (Figure 8). The tumor-to-kidney absorbed dose ratio of [^{177}Lu]Lu-Albutate-1 is 1.5 ± 0.5. The tumor-to-pancreas absorbed dose ratio is 3.9 ± 0.4 and the tumor-to-bone marrow absorbed dose ratio is 2.4 ± 0.9.

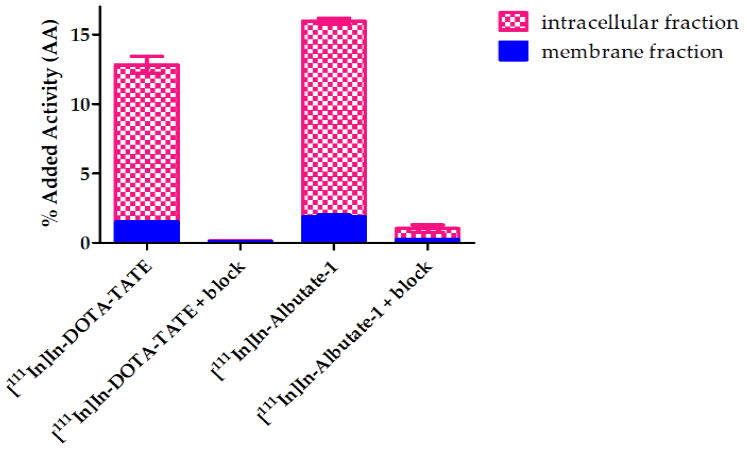

Figure 5: Uptake and internalization of [^{111}In]In-Albutate-1 and [^{111}In]In-DOTA-TATE in U2OS-SSTR2 cells.

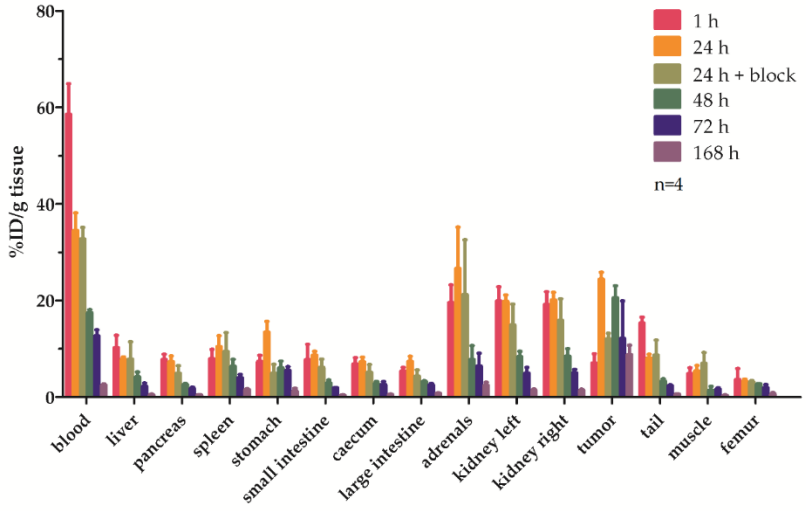

Figure 6: Biodistribution of [^{177}Lu]Lu-Albutate-1 in blood, organs and tumor. 30 MBq/240 pmol [^{177}Lu]Lu-Albutate-1 (for 24h +/- block) was injected i.v. in mice and biodistribution was determined at 1, 24, 48, 72 and 168 h after injection (n=4 per group). The amount of radioactivity in the tissue samples was determined and calculated per gram.

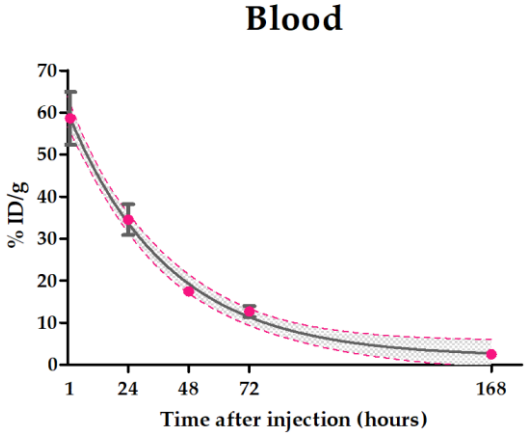

Figure 7: Blood residence of [^{177}Lu]Lu-Albutate-1 as a function of time (n=4). The Albutate-1 data was fitted (R^2=0.98) with a one phase decay curve with T_{clr} = 27.5 ± 2.6 h. The error bars indicate 1 standard deviation and the shaded regions indicate the 95% confidence interval.

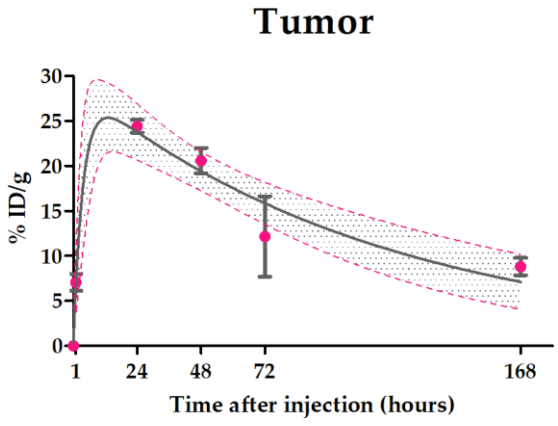

Figure 8: Tumor uptake of [^{177}Lu]Lu-Albutate-1 as a function of time (n = 4). The Albutate-1 data was fitted (R^2=0.87) with a bi-exponential curve with T_{upt} = 2.52 ± 0.98 h and T_{clr} = 80 ± 19 h. Error bars indicate 1 standard deviation and 95% confidence interval of the fits are indicated.

V Dosimetry

All organ time-activity curves could be fitted with an exponential function for parameters and goodness of fits. The blood curve of [^{177}Lu]Lu-Albutate-1 followed a single exponential clearance pattern with $T_{1/2}$ = 27.5 ± 2.6 h. The blood concentration and the total number of disintegrations in the bone marrow cavities were calculated (Table 1). In (Table 2), the absorbed dose per administered activity to the major organs is described. SSTR2 positive organs (such as intestines, pancreas, adrenals, etc.) encountered a high absorbed dose per administered activity.

Table 1: Dosimetry to bone marrow cavities, CF cellularity factor, time-integrated activity coefficient of blood in BM compartment $\tilde{A}_{blood}$/IA, blood self-dose D_{self} and cross dose D_{cross} by activity in other organs, both per injected activity IA.

	CF	$\tilde{A}_{blood}$/IA (s)	D_{self}/IA (mGy/MBq)	D_{cross} /IA (mGy/MBq)
Sternum	8%	41	104	24
Spine	52%	6617	741	27
Skull	11%	499	170	26
Ribs	8%	142	81	47
Arms	5%	76	74	15
Lower legs	4%	118	67	11
Pelvis	7%	272	108	29
Scapulae	3%	31	42	43
Femurs	10%	171	169	58

Table 2: Absorbed dose per administered activity to the major organs in 22g weight mice for [^{177}Lu]Lu-Albutate-1.

	mGy/MBq
Tumor	1455
Adrenals	1073
Kidney	958
BM spine	765
Intestines	566
Spleen	538
Liver	422
Pancreas	373
Total body	253
Stomach	247
Femur	211

Discussion

For optimization of the therapeutic efficacy of the currently used [^{177}Lu]Lu-DOTA-TATE therapy for NETs, we chose to enhance the circulation time of the radiotracer. An albumin binding domain, 4-(p-iodophenyl) butyric acid-DLys, was covalently coupled to TATE via a diglycolic acid-Lys (DOTA) linker. The latter bears the chelator DOTA attached to the free ε-amine of Lys. The forming TATE conjugate, Albutate-1, is depicted in (Figure 1). In this study, we evaluated Albutate-1 in *in vitro* and *in vivo* studies in mice. DOTA-TATE and Albutate-1 showed a comparable binding affinity for SSTR2 (IC_{50} 0.2-1.6 nM), so the attachment of an albumin-binding domain did not affect SSTR2 binding [35, 36]. The cell uptake and internalization of [^{111}In]In-Albutate-1 and [^{111}In]In-DOTA-TATE were similar as well. Most radioactivity was found in the intracellular fraction (88%), so the addition of the albumin-binding moiety did not hamper the internalization of the tracer. Biodistribution studies were performed at 5 different time points after injection of [^{177}Lu]Lu-Albutate-1 (30 MBq/240 pmol).

The activity level of [^{177}Lu]Lu-Albutate-1 in the blood was 58.59 ± 6.30%ID/g at 1h and gradually decreased down to 2.51 ± 0.22%ID/g at 168 h. The measured tumor uptake was the highest 24 h post-injection, 24.42 ± 1.44%ID/g. So, *in vivo* we found that the half-life of [^{177}Lu]Lu-Albutate-1 was 27.5 ± 2.6 h in blood which is longer when compared to [^{177}Lu]Lu-DOTA-TATE that has disappeared from blood within 4h [37]. To block the SSTR2, four mice were injected with 50 ug Albutate-1.

The reduced uptake in the SSTR2 positive organs and tumor indicates that in these mice, the [^{177}Lu]Lu-Albutate-1 binding is specific to the receptor. Since the radioactive dose to normal organs is of utmost importance during radionuclide therapy, we performed extensive dosimetry calculations. We noticed that there was a tumor absorbed dose per administered activity of 1455 mGy/MBq. Normal organs however, also encountered a higher absorbed dose, especially bone marrow. We calculated that the spine, which has a cellular fraction 52%, received a total absorbed dose of 765 mGy/MBq. The blood circulation time is extended, compared to [^{177}Lu]Lu-DOTA-TATE and therefore, the high normal organ exposure of [^{177}Lu]Lu-DOTA-Albutate-1 is reducing the therapeutic index [13]. At a limiting dose to the bone marrow of 2 Gy only a 14 Gy absorbed dose to the tumor can be reached, together with an absorbed dose to the kidneys of 9 Gy. Looking at our data, we propose to make adjustments to further improve our albumin binding tracer concept. Like us, other groups also tried to prolong the blood circulation time of their tracer.

A search for enhancing the tumor uptake and improving the tumor-to-kidney ratio took place [38]. They also searched for the best balance between high tumor dose and limited organ dose. The structure of the tracer can be modified by varying the binding strength to albumin and/or varying the spacer length. Rousseau *et al.* conjugated two different albumin binders, Lys-Glu-4-(p-iodophenyl) butyric acid or Lys-Asp-4-(p-iodophenyl) butyric acid, to the parent compound DOTA-TATE [39]. The addition of these albumin binders increased blood residence time, in tumor-bearing mice, by a couple of hours. Although their tracer with Asp-4-(p-iodophenyl) butyric acid as albumin binder has a more modest increase of circulation time than our [^{177}Lu]Lu-Albutate-1 ($t_{1/2}$ ~ 3 vs 27 h), also no increase in the therapeutic index was seen. Indicating that the albumin binder should not bind too strong and not too weak.

Műller *et al.* performed preclinical research and found that adding the 4-(p-iodophenyl) butyric acid albumin-binding entity to a DOTA-folate improved the overall tissue distribution significantly [22]. To further reduce the renal accumulation of radioactivity, the same group also made two other albumin-binding radiofolates to further restrict renal accumulation [40, 41]. A longer spacer consisting of a PEG-11 entity and a short alkyl chain between the albumin-binding moiety and folic acid was investigated [21]. Data shows that the spacer entity between folic acid and the albumin binder was of critical importance with regard to the tissue distribution profile of the radiotracer, with a preference for

a shorter spacer entity. Knowing this, we have to take another look at our spacer.

The same group studied three different prostate-specific membrane antigen (PSMA) targeting radioligands with a 4-(p-iodophenyl)-based albumin binder, the same as applied in our study. They developed three ligands with variations in linker length [42]. All radioligands showed an enhanced circulation time and a higher tumor uptake, but the one with the shortest linker length emerged as the most favourable candidate of all ligands, which might be promising for our approach as well. In another study, albumin binders were based on a stronger albumin-binding 4-(p-iodophenyl)-moiety and a weaker albumin-binding p-(tolyl)-moiety [43]. The weaker albumin-binder affected tumor uptake, blood retention time and the therapeutic index more positively, pointing out to be more suited as an albumin binder with an optimized tissue distribution profile. A weaker albumin binder than we have attached has to be used for the new to develop compounds.

Evans Blue (EB) is a compound that can also be used as an albumin binder. EB and its analogs exhibit a modest affinity for serum albumin. R. Tian *et al*. describe the addition of EB to DOTA-TATE and performed a mouse biodistribution and therapy study [15]. This research was continued with a small in-patient study [16]. [^{177}Lu]Lu-EB-DOTA-TATE showed a 7.9-fold increase of tumor dose delivery and higher retention in NETs compared to [^{177}Lu]Lu-DOTA-TATE, but there was also a significantly increased accumulation in the kidneys (3.2 fold) and red marrow (18.2 fold). This single low dose treatment of [^{177}Lu]Lu-EB-DOTA-TATE in a small group of patients seemed to be safe and effective. Further investigation with increased dose and frequency is needed to determine the potential advantages of a longer circulating tracer [44]. So, according to our results and the above-mentioned literature, albumin binders attached to tracers can improve circulation time and increase tumor uptake. If the plasma protein-binding takes a long time to reverse, the blood circulation time is extended to a level that all other organs also receive a high radiation dose, reducing the therapeutic index dramatically. Future perspectives are to create a tracer with more optimal pharmacokinetics, applying adaptations in albumin binding strength, spacer length and lipophilicity.

Conclusion

The addition of an albumin-binding domain to [^{177}Lu]Lu-DOTA-TATE extended the blood circulation to $t_{1/2}$= 27.5h. The tumor absorbed dose is raised to 1455 mGy/Bq. The bone marrow of the mouse spine, as dose-limiting organ, received 765 mGy/MBq. All other organs also received a high radiation dose, reducing the therapeutic index. Making Albutate-1 not suitable to use as a therapeutic agent.

Acknowledgement

All imaging experiments were conducted at the Applied Molecular Imaging at Erasmus MC Facility.
(https://www.erasmusmc.nl/en/research/core-facilities/amie)

Conflicts of Interest

None.

References

1. Fraenkel M, Kim M, Faggiano A, de Herder WW, Valk GD et al. (2014) Incidence of gastroenteropancreatic neuroendocrine tumours: a systematic review of the literature. *Endocr Relat Cancer* 21: R153-R163. [Crossref]
2. Korse CM, Taal BG, van Velthuysen ML, Visser O (2013) Incidence and survival of neuroendocrine tumours in the Netherlands according to histological grade: experience of two decades of cancer registry. *Eur J Cancer* 49: 1975-1983. [Crossref]
3. Pauwels E, Cleeren F, Bormans G, Deroose CM (2018) Somatostatin receptor PET ligands - the next generation for clinical practice. *Am J Nucl Med Mol Imaging* 8: 311-331. [Crossref]
4. Waldmann CM, Stuparu AD, van Dam RM, Slavik R (2019) The Search for an Alternative to [(68)Ga]Ga-DOTA-TATE in Neuroendocrine Tumor Theranostics: Current State of (18)F-labeled Somatostatin Analog Development. *Theranostics* 9: 1336-1347. [Crossref]
5. Severi S, Grassi I, Nicolini S, Sansovini M, Bongiovanni A et al. (2017) Peptide receptor radionuclide therapy in the management of gastrointestinal neuroendocrine tumors: efficacy profile, safety, and quality of life. *Onco Targets Ther* 10: 551-557. [Crossref]
6. Hennrich U, Kopka K (2019) Lutathera®: The First FDA- and EMA-Approved Radiopharmaceutical for Peptide Receptor Radionuclide Therapy. *Pharmaceuticals* 12: 114. [Crossref]
7. Kolasinska Cwikla A, Peczkowska M, Cwikla JB, Michalowska I, Palucki JM et al. (2019) A Clinical Efficacy of PRRT in Patients with Advanced, Nonresectable, Paraganglioma-Pheochromocytoma, Related to SDHx Gene Mutation. *J Clin Med* 8: 952. [Crossref]
8. Bodei L, Kwekkeboom DJ, Kidd M, Modlin IM, Krenning EP (2016) Radiolabeled Somatostatin Analogue Therapy of Gastroenteropancreatic Cancer. *Semin Nucl Med* 46: 225-238. [Crossref]
9. Kwekkeboom DJ, De Herder WW, Kam BL, van Eijck CH, van Essen M et al. (2008) Treatment With the Radiolabeled Somatostatin Analog [177Lu-DOTA0,Tyr3]Octreotate: Toxicity, Efficacy, and Survival. *J Clin Oncol* 26: 2124-2130. [Crossref]
10. Kwekkeboom DJ, Kam BL, van Essen M, Teunissen JJ, van Eijck CH et al. (2010) Somatostatin-receptor-based imaging and therapy of gastroenteropancreatic neuroendocrine tumors. *Endocr Relat Cancer* 17: R53-R73. [Crossref]
11. Rolleman EJ, Melis M, Valkema R, Boerman OC, Krenning EP et al. (2010) Kidney protection during peptide receptor radionuclide therapy with somatostatin analogues. *Eur J Nucl Med Mol Imaging* 37: 1018-1031. [Crossref]
12. Melis M, Bijster M, de Visser M, Konijnenberg MW, de Swart J et al. (2009) Dose-response effect of Gelofusine on renal uptake and retention of radiolabelled octreotate in rats with CA20948 tumours. *Eur J Nucl Med Mol Imaging* 36: 1968-1976. [Crossref]
13. Esser JP, Krenning EP, Teunissen JJ, Kooij PP, van Gameren AL et al. (2006) Comparison of [(177)Lu-DOTA(0),Tyr(3)]octreotate and [(177)Lu-DOTA(0),Tyr(3)]octreotide: which peptide is preferable for PRRT? *Eur J Nucl Med Mol Imaging* 33: 1346-1351. [Crossref]
14. Kratz F (2008) Albumin as a drug carrier: design of prodrugs, drug conjugates and nanoparticles. *J Control Release* 132: 171-183. [Crossref]

15. Tian R, Jacobson O, Niu G, Kiesewetter DO, Wang Z et al. (2018) Evans Blue Attachment Enhances Somatostatin Receptor Subtype-2 Imaging and Radiotherapy. *Theranostics* 8: 735-745. [Crossref]
16. Zhang J, Wang H, Jacobson O, Cheng Y, Niu G et al. (2018) Safety, Pharmacokinetics and Dosimetry of a Long-Acting Radiolabeled Somatostatin Analogue (177)Lu-DOTA-EB-TATE in Patients with Advanced Metastatic Neuroendocrine Tumors. *J Nucl Med* 59: 1699-1705. [Crossref]
17. Wang Z, Tian R, Niu G, Ma Y, Lang L et al. (2018) Single Low-Dose Injection of Evans Blue Modified PSMA-617 Radioligand Therapy Eliminates Prostate-Specific Membrane Antigen Positive Tumors. *Bioconjug Chem* 29: 3213-3221. [Crossref]
18. Dumelin CE, Trussel S, Buller F, Trachsel E, Bootz F et al. (2008) A portable albumin binder from a DNA-encoded chemical library. *Angew Chem Int Ed Engl* 47: 3196-3201. [Crossref]
19. Muller C, Farkas R, Borgna F, Schmid RM, Benesova M et al. (2017) Synthesis, Radiolabeling, and Characterization of Plasma Protein-Binding Ligands: Potential Tools for Modulation of the Pharmacokinetic Properties of (Radio)Pharmaceuticals. *Bioconjug Chem* 28: 2372-2383. [Crossref]
20. Trussel S, Dumelin C, Frey K, Villa A, Buller F et al. (2009) New strategy for the extension of the serum half-life of antibody fragments. *Bioconjug Chem* 20: 2286-2292. [Crossref]
21. Siwowska K, Haller S, Bortoli F, Benesova M, Groehn V et al. (2017) Preclinical Comparison of Albumin-Binding Radiofolates: Impact of Linker Entities on the in Vitro and in Vivo Properties. *Mol Pharm* 14: 523-532. [Crossref]
22. Muller C, Struthers H, Winiger C, Zhernosekov K, Schibli R (2013) DOTA conjugate with an albumin-binding entity enables the first folic acid-targeted 177Lu-radionuclide tumor therapy in mice. *J Nucl Med* 54: 124-131. [Crossref]
23. Kelly JM, Amor Coarasa A, Nikolopoulou A, Wustemann T, Barelli P et al. (2017) Dual-Target Binding Ligands with Modulated Pharmacokinetics for Endoradiotherapy of Prostate Cancer. *J Nucl Med* 58: 1442-1449. [Crossref]
24. Choy CJ, Ling X, Geruntho JJ, Beyer SK, Latoche JD et al. (2017) ^{177}Lu-Labeled Phosphoramidate-Based PSMA Inhibitors: The Effect of an Albumin Binder on Biodistribution and Therapeutic Efficacy in Prostate Tumor-Bearing Mice. *Theranostics* 7: 1928-1939. [Crossref]
25. Breeman WA, De Jong M, Visser TJ, Erion JL, Krenning EP (2003) Optimising conditions for radiolabelling of DOTA-peptides with 90Y, 111In and 177Lu at high specific activities. *Eur J Nucl Med Mol Imaging* 30: 917-920. [Crossref]
26. Bakker WH, Albert R, Bruns C, Breeman WA, Hofland LJ et al. (1991) [111In-DTPA-D-Phe1]-octreotide, a potential radiopharmaceutical for imaging of somatostatin receptor-positive tumors: synthesis, radiolabeling and in vitro validation. *Life Sci* 49: 1583-1591. [Crossref]
27. Dalm SU, Nonnekens J, Doeswijk GN, de Blois E, van Gent DC et al. (2016) Comparison of the Therapeutic Response to Treatment with a 177Lu-Labeled Somatostatin Receptor Agonist and Antagonist in Preclinical Models. *J Nucl Med* 57: 260-265. [Crossref]
28. Kilkenny C, Browne WJ, Cuthill IC, Emerson M, Altman DG (2010) Improving bioscience research reporting: the ARRIVE guidelines for reporting animal research. *PLoS Biol* 8: e1000412. [Crossref]
29. De Jong M, Valkema R, Jamar F, Kvols LK, Kwekkeboom DJ et al. (2002) Somatostatin receptor-targeted radionuclide therapy of tumors: preclinical and clinical findings. *Semin Nucl Med* 32: 133-140. [Crossref]
30. Bison SM, Pool SE, Koelewijn SJ, van der Graaf LM, Groen HC et al. (2014) Peptide receptor radionuclide therapy (PRRT) with [(177)Lu-DOTA(0),Tyr(3)]octreotate in combination with RAD001 treatment: further investigations on tumor metastasis and response in the rat pancreatic CA20948 tumor model. *EJNMMI Res* 4: 21. [Crossref]
31. Breeman WA, van der Wansem K, Bernard BF, van Gameren A, Erion JL et al. (2003) The addition of DTPA to [177Lu-DOTA0,Tyr3]octreotate prior to administration reduces rat skeleton uptake of radioactivity. *Eur J Nucl Med Mol Imaging* 30: 312-315. [Crossref]
32. Chan HS, Konijnenberg MW, Daniels T, Nysus M, Makvandi M et al. (2016) Improved safety and efficacy of (213)Bi-DOTATATE-targeted alpha therapy of somatostatin receptor-expressing neuroendocrine tumors in mice pre-treated with L-lysine. *EJNMMI Res* 6: 83. [Crossref]
33. Larsson E, Strand SE, Ljungberg M, Jonsson BA (2007) Mouse S-factors based on Monte Carlo simulations in the anatomical realistic Moby phantom for internal dosimetry. *Cancer Biother Radiopharm* 22: 438-442. [Crossref]
34. Colvin GA, Lambert JF, Abedi M, Hsieh CC, Carlson JE et al. (2004) Murine marrow cellularity and the concept of stem cell competition: geographic and quantitative determinants in stem cell biology. *Leukemia* 18: 575-583. [Crossref]
35. Reubi JC, Schar JC, Waser B, Wenger S, Heppeler A et al. (2000) Affinity profiles for human somatostatin receptor subtypes SST1-SST5 of somatostatin radiotracers selected for scintigraphic and radiotherapeutic use. *Eur J Nucl Med* 27: 273-282. [Crossref]
36. Bodei L, Mueller Brand J, Baum RP, Pavel ME, Horsch D et al. (2018) The joint IAEA, EANM, and SNMMI practical guidance on peptide receptor radionuclide therapy (PRRNT) in neuroendocrine tumours. *Eur J Nucl Med Mol Imaging* 40: 800-816. [Crossref]
37. de Jong M, Breeman WA, Bernard BF, Bakker WH, Schaar M et al. (2001) [177Lu-DOTA(0),Tyr3] octreotate for somatostatin receptor-targeted radionuclide therapy. *Int J Cancer* 92: 628-633. [Crossref]
38. Lau J, Jacobson O, Niu G, Lin KS, Benard F et al. (2019) Bench to Bedside: Albumin Binders for Improved Cancer Radioligand Therapies. *Bioconjug Chem* 30: 487-502. [Crossref]
39. Rousseau E, Lau J, Zhang Z, Uribe CF, Kuo HT et al. (2018) Effects of adding an albumin binder chain on [(177)Lu]Lu-DOTATATE. *Nucl Med Biol* 66: 10-17. [Crossref]
40. Vegt E, de Jong M, Wetzels JF, Masereeuw R, Melis M et al. (2010) Renal toxicity of radiolabeled peptides and antibody fragments: mechanisms, impact on radionuclide therapy, and strategies for prevention. *J Nucl Med* 51: 1049-1058. [Crossref]
41. Farkas R, Siwowska K, Ametamey SM, Schibli R, van der Meulen NP et al. (2016) (64)Cu- and (68)Ga-Based PET Imaging of Folate Receptor-Positive Tumors: Development and Evaluation of an Albumin-Binding NODAGA-Folate. *Mol Pharm* 13: 1979-1987. [Crossref]
42. Benesova M, Umbricht CA, Schibli R, Muller C (2018) Albumin-Binding PSMA Ligands: Optimization of the Tissue Distribution Profile. *Mol Pharm* 15: 934-946. [Crossref]
43. Umbricht CA, Benesova M, Schibli R, Muller C (2018) Preclinical Development of Novel PSMA-Targeting Radioligands: Modulation of

Albumin-Binding Properties To Improve Prostate Cancer Therapy. *Mol Pharm* 15: 2297-2306. [Crossref]

44. Wang H, Cheng Y, Zhang J, Zang J, Li H et al. (2018) Response to Single Low-dose (177)Lu-DOTA-EB-TATE Treatment in Patients with Advanced Neuroendocrine Neoplasm: A Prospective Pilot Study. *Theranostics* 8: 3308-3316. [Crossref]